Template for engineering journal articles

- Article type: paper (3000-5000 words, excluding abstract and References list)
- One illustration per 500 words.
- **Date text written or revised.**
- Number of words in your main text and tables, followed by the number of figures.
- This is an example created from parts of other articles; it is not designed to be read for sense.
- Text should be double line spaced, line numbered and pages should be numbered.

Title (maximum length of 90 characters including spaces)

Probabilistic Long-Term Resilience of Bridges under Seismic and Deterioration Processes

Author 1

- Jing Qian, Research assistant and PhD student
- Department of Civil and Environmental Engineering, The Hong Kong Polytechnic University, Hong Kong, China, jingce.qian@connect.polyu.hk
- ORCID number: 0000-0003-4617-3161

Author 2

- You Dong, Assistant Professor of Structural Engineering
- Department of Civil and Environmental Engineering, The Hong Kong Polytechnic University, Hong Kong, China, you.dong@polyu.edu.hk
- ORCID number: 0000-0002-2499-0999

Author 3

- Dan M. Frangopol, Professor and the Fazlur R. Khan Endowed Chair of Structural Engineering and Architecture
- Department of Civil and Environmental Engineering, Engineering Research Center for Advanced Technology for Large Structural Systems (ATLSS Center), Lehigh University, 117 ATLSS Dr., Bethlehem, PA 18015-4729, USA, dan.frangopol@lehigh.edu, corresponding author
- ORCID number: 0000-0002-9213-0683

Full contact details of corresponding author.

Abstract (150 – 200 words)

Accurate long-term risk and resilience assessment of bridges are of paramount importance to aid rational decision-making under seismic hazards. There exist time-varying features within both earthquakes and structural deterioration. It has been found that the occurrence of large earthquakes is dependent on time due to energy accumulation, whereas the widely adopted homogeneous Poisson process assumes the time-independent occurrence of hazards. Besides, bridges can deteriorate over time due to environmental exposure, resulting in increased seismic vulnerability. The time-varying characteristics associated with both earthquakes and deterioration, which cause compound effects to structures, should be incorporated in long-term seismic risk and resilience assessment. In this paper, an approach for assessing the long-term resilience of bridges incorporating time-varying characteristics of earthquakes and deterioration is proposed. The Brownian Passage Time (BPT) model capturing energy accumulation and release is used to model time-varying characteristics of earthquakes. The bridge seismic vulnerability is computed in a time-variant manner considering deterioration. Subsequently, long-term bridge resilience is computed by considering earthquakes and deterioration occurring during the entire service life of bridges. The proposed approach is illustrated on a highway bridge under time-dependent seismic hazard and structural deterioration.

Keywords chosen from ICE Publishing list

Seismic engineering; Resilience; Corrosion; Risk & probability analysis.

List of notations

$a(t)$	coefficient of the demand prediction model at time t
$A_{DP}(t)$	residual area of pit excluding uniform corrosion at time t (mm^2)
$b(t)$	coefficient of the demand prediction model at time t
BPT	Brownian Passage Time
C_{cr}	critical chloride concentration (% weight of concrete)
C_s	equilibrium chloride concentration at the concrete surface (% weight of concrete)
$D_{cl,0}$	reference diffusion coefficient (cm^2/year)
D_C	diffusion coefficient for the deicing salt environment (cm^2/year)
D_i	diameter of pristine reinforcing steel (mm)
erf	Gaussian error function
F_E	function of earthquake source
F_P	function of earthquake path
F_S	function of earthquake site
$F(IM\|t, DS)$	fragility of the structure under *IM* and damage state *DS* at time t
GMPM	ground motion prediction model
HPP	homogeneous Poisson process

71	$i_{corr}(0)$	initial corrosion rate in current density ($\mu A/cm^2$)
72	IM	seismic intensity measure (g)
73	k_c	curing factor
74	k_e	environmental factor
75	$\ln Y$	natural logarithm of ground motion intensity
76	L_R	long-term resilience loss
77	*mech*	earthquake mechanism
78	M	moment magnitude of the event
79	n_{cl}	variable incorporating the densification of material
80	$N_h(t_L)$	number of hazards within the investigated time horizon t_L
81	$p(t)$	pit depth at time t (mm)
82	PDF	probability density function
83	$Q(t\|t_i)$	post-hazard time-variant functionality of the system under the earthquake
84	accruing at time t_i	
85	r_{corr}	initial corrosion rate (mm/year)
86	$r_{corr}(t_p)$	mean corrosion rate at the time t_p after initiating corrosion (mm/year)
87	*region*	region of the earthquake accruing
88	R	pitting factor
89	R_{JB}	Joyner-Boore distance (km)
90	$R_L(t_i)$	resilience loss index caused by the earthquake at time t_i
91	$S_d(t,IM)$	median of seismic demand under given time t and IM (cm if the demand
92	is displacement)	
93	STD	standard deviation
94	t_0	concrete age at the time of conducting compliance test (years)
95	t_h	investigated recovery time horizon (days)
96	t_L	investigated time horizon of long-term resilience (years)
97	T_i	time of corrosion initiation for a specific scenario (years)
98	V_{S30}	shear wave velocity averaged over top 30 m (m/s)
99	V_{ti}	vulnerability of structures at the time of t_i
100	$w_p(t)$	width of the pit excluding uniform corrosion at time t (mm)
101	w/c	water-cement ratio of concrete material
102	W_i	inter-arrival time of the earthquake (years)
103	x	depth of cover concrete (cm)
104	z_1	basin depth (km)
105	α	coefficient of variation of the BPT model
106	$\beta_{0,DS}(t)$	coefficient of the fragility model at time t
107	$\beta_{IM,DS}(t)$	coefficient of the fragility model at time t
108	λ	annual occurrence rate of the event
109	σ	standard deviation of the ground motion intensity
110	ε	fractional number of standard deviations of the value of $\ln Y$ away from
111	the mean	

μ	mean value of the BPT model (years)

1. Introduction

Highway bridges represent an essential transportation infrastructure for economic and social activities. Within the service life, bridges can suffer continuous deterioration due to corrosion and sudden disruptions due to extreme events such as earthquakes, resulting in severe social and economic consequences. From a long-term perspective, these consequences can be accumulated due to multiple disruptions. To ensure the safety and functionality of bridges within their prescribed service life, it is of vital importance to understand the long-term resilience of bridges under both continuous deterioration and extreme events. Within the service life of structures, earthquakes can occur with stochastic occurrence time and intensity. The occurrence of earthquakes can be modelled using stochastic process models (Pandey and Van Der Weide, 2017). The homogeneous Poisson process (HPP) is widely adopted for computing long-term damage costs (Liu, Wen and Burns, 2004). In HPP, the mean occurrence rate is assumed to be constant, and the occurrence of hazards is considered as independent from time (Takahashi, Der Kiureghian and Ang, 2004). The simplicity of HPP may not well capture stochastic characteristics of hazards (Pandey and Van Der Weide, 2017). Due to the mechanism of energy accumulation and release, the occurrence of earthquakes is associated with time-dependent features (Matthews, Ellsworth and Reasenberg, 2002). For instance, the earthquake can occur when energy accumulation meets a critical state. The energy is released after the earthquake, and a new cycle of rupture failure starts. Considering time-dependent characteristics, the Brownian passage-time (BPT) renewal process can be used to model the long-term occurrence of earthquakes (Matthews, Ellsworth and Reasenberg, 2002; Li, Dong, Dan M Frangopol, *et al.*, 2020). The time-dependent seismic renewal process model has not been well incorporated in the long-term performance and resilience assessment of structures.

Bridges can be exposed to chloride environments. Chloride can penetrate concrete cover and contact reinforcing steel initiating corrosion (Stewart and Al-Harthy, 2008). The corrosion causes area loss of reinforcing steel and other secondary effects on structures, leading to time-variant capacity. Deterioration is associated with time-variant characteristics, and it can continuously increase the damage probability of bridges under earthquakes. Ghosh and Padgett (2010) developed time-variant fragility curves considering corrosion. Then, the framework of

seismic life-cycle cost assessment incorporating corrosion was developed (Shekhar, Ghosh and Padgett, 2018). The deterioration process has not been well incorporated into the framework of long-term seismic resilience assessment.

Resilience has received increasing attention in the decision-making process regarding structural systems. Resilience is defined as the ability of systems to absorb disruptions and recover to a satisfying functionality state (Timmerman, 1981). Frangopol and Bocchini (2011) defined resilience index as the ratio of integration of time-variant functionality over investigated time horizon to the total investigated time. Decò, Bocchini and Frangopol, (2013) developed a probabilistic approach to quantify the time-variant functionality and resilience of bridges considering uncertainties within the recovery process. Dong and Frangopol (2016) developed a framework to assess the seismic resilience of bridges under flood effects. Minaie and Moon (2017) developed a multistage framework to assess the resilience of bridges by incorporating expert knowledge and lessons from previous experience. The effects of different seismic intensity measures (IM) on probabilistic resilience have been assessed to support IM selection (Qian and Dong, 2020). Most of the studies on seismic resilience only focus on a single hazard, Dong and Frangopol (2015) proposed a framework to quantify seismic resilience under mainshock and aftershock sequences. Kong and Simonovic (2019) developed an approach for assessing the resilience of infrastructure systems considering interdependence among infrastructure systems, multiple hazard interactions, and restoration strategies. Argyroudis *et al.* (2020) proposed a framework to quantify the resilience of infrastructure under multiple hazards incorporating vulnerability, recovery rapidity, and temporal variability. The studies on long-term seismic resilience assessment are limited. Yang and Frangopol (2019) introduced the concept of lifetime resilience and approaches based on the stochastic process were developed to assess lifetime resilience. Li *et al.* (2020) developed a framework for assessing long-term resilience under multiple natural hazards. The corrosion process can escalate the seismic vulnerability of structures and affect long-term seismic resilience. The seismic resilience of structures at different times was assessed considering deterioration (Capacci and Biondini, 2020). The seismic resilience loss can be accumulated within the service life of deteriorating structures, due to the occurrence of multiple earthquakes and continuous corrosion.

Overall, the long-term resilience assessment framework incorporating both deterioration and time-dependent seismic processes has not been well developed. Specifically, the corrosion process has not been coupled with the seismic process for assessing accumulated seismic resilience loss within the service life of structures. Additionally, the effects of different stochastic processes of deterioration and earthquake on statistical moments of resilience have not been investigated. To address these issues, this study proposes a framework for long-term resilience assessment considering seismic and deterioration processes. The seismic process is coupled with the corrosion process to assess long-term accumulated resilience loss within the service life of structures. The time-dependent features within deterioration and seismic processes are considered for computing time-dependent fragility and modelling the occurrence of earthquakes, respectively. The uncertainties associated with hazard intensity, hazard occurrence time, structural damage, and corrosion can be incorporated in the developed framework.

The remainder of this paper is organized as follows. The deterioration process of structures is introduced in section 2. The seismic processes are presented in section 3. The developed long-term resilience assessment framework is illustrated in Section 4. An illustrative example is presented in Section 5. Section 6 contains a summary and conclusions.

2. Deterioration process

To assess seismic vulnerability and resilience from a long-term perspective, understanding the mechanism of deterioration is necessary. The deterioration is a continuous process occurring within the service life of structures. The corrosion induced by the chloride exposure environment can continuously affect the performance and resilience of structures (Akiyama, Frangopol and Ishibashi, 2020).

2.1 Chloride exposure environment

The following considerations apply for boxes (1) and (2) in Figure 2. The practical chloride exposure conditions typically include marine atmospheric environment, marine splash environment, and deicing salt environment (Ghosh and Padgett, 2012). Corrosion initiation time and rate of corrosion under these three exposure conditions are introduced in this study.

Coastal bridges are exposed to the marine environment. Due to the existence of capillary pores within concrete material, suction of chloride solution in concrete structural components can happen. Then, the concentration of chlorides can be increased from water evaporation and corrosion is initiated when these chlorides penetrate through cover concrete and contact with steel (Choe *et al.*, 2008; Shekhar, Ghosh and Padgett, 2018). A diffusion model can be adopted to compute corrosion initiation time $T_{i,marine}$ with respect to marine exposure as (Engelund, Edvardsen and Mohr, 2000)

$$T_{i,marine} = \left\{ \frac{x^2}{4k_e k_c D_{cl,0} (t_0)^{n_{cl}}} \left[erf^{-1} \left(\frac{C_s - C_{cr}}{C_s} \right) \right]^{-2} \right\}^{\frac{1}{(1-n_{cl})}} \quad (1)$$

where x is the depth of cover concrete; $D_{cl,0}$ represents reference diffusion coefficient; k_c is the curing factor; k_e represents the environment factor; t_0 is the concrete age at the time of conducting compliance test; n_{cl} is the variable incorporating the densification of material; C_s represents the equilibrium chloride concentration at the concrete surface; C_{cr} is the critical chloride concentration; and the *erf* is the Gaussian error function.

After the initiation of corrosion, the area of steel starts to reduce. The corrosion rate is associated with uncertainties and it depends on different environments (Frangopol, Lin and Estes, 1997). A time-variant corrosion rate model under marine exposure is expressed as (Vu and Stewart, 2000)

$$r_{corr}(0) = 0.0116 i_{corr}(0) = 0.0116 \times \frac{37.8(1 - w/c)^{-1.64}}{x} \quad (2)$$

$$r_{corr}(t_p) = 0.85 r_{corr}(0) t_p^{-0.29} \quad (3)$$

where $i_{corr}(0)$ is the initial corrosion rate in current density (in the unit of μA/cm^2); w/c is the water-cement ratio of concrete material; $r_{corr}(0)$ is the initial corrosion rate (in the unit of mm/year), and $r_{corr}(t_p)$ is the mean corrosion rate at the time t_p after initiating corrosion.

In addition to marine atmospheric and marine splash environment, structures can be exposed to deicing salt. For the transportation networks located in frozen regions, deicing salts are spread on road networks to eliminate snow to ensure operational safety. Compared with the

marine environment, deicing salt can normally cause severer corrosion of structures due to its higher content of chlorides (Ghosh and Padgett, 2010). The corrosion initiation time with respect to deicing salt environment can be expressed as (Enright and Frangopol, 1998)

$$T_{i,deicing} = \frac{x^2}{4D_C}\left[erf^{-1}\left(\frac{C_s - C_{cr}}{C_s}\right)\right]^{-2} \tag{4}$$

where D_C is the diffusion coefficient for the deicing salt environment. The corrosion rate for this environment can be obtained from experiments and observational measurements. The probabilistic distribution of corrosion rate under deicing salt environment can be found in Enright and Frangopol (1998).

2.2 Effects of corrosion

The following considerations apply for the box (3) in Figure 2. The effects of corrosion within reinforced concrete structures can be summarized as area reduction of steel and secondary effects. After the chlorides penetrate the concrete cover and contact with steel, area loss of steel commences. Uniform corrosion and pitting corrosion are two widely adopted models to characterize the area loss of steel. For uniform corrosion, area loss of reinforcing steel is considered as uniform around the circumference of reinforcing steel. Under this consideration, the residual area of rebar can be computed as (Enright and Frangopol, 1998; Shekhar, Ghosh and Padgett, 2018)

$$A_U(t) = \begin{cases} \frac{\pi}{4} D_i^2 & \text{for } t \le T_i \\ \frac{\pi}{4}\left[D_i - 2\int_{T_i}^{t} r_{corr}(t_p)dt_p \right]^2 & \text{for } 2\int_{T_i}^{t} r_{corr}(t_p)dt_p < D_i \\ 0 & \text{for } D_i \le 2\int_{T_i}^{t} r_{corr}(t_p)dt_p \end{cases} \tag{5}$$

where D_i is the diameter of pristine reinforcing steel and T_i represents the time of corrosion initiation for a specific scenario.

In addition to uniform corrosion, deep pits along the length of corroded reinforcing steel were reported in previous studies. The area loss due to pitting corrosion can be significantly

larger than the area loss induced by uniform corrosion (Zandi Hanjari, Kettil and Lundgren, 2011). Thus, pitting corrosion should be appropriately modelled within the corrosion process accompanied by uniform corrosion. The residual rebar area subjected to pitting corrosion can be computed using a hemispherical pit model as follows (Ghosh and Sood, 2016)

$$A_p(t) = \left[1 - \frac{w_p(t)}{2D_i}\right]\left[A_U(t) - \frac{\pi}{4}D_i^2\right] + A_{DP}(t) \quad (6)$$

where $w_p(t)$ is the width of the pit excluding uniform corrosion; and $A_{DP}(t)$ is the residual area of pit excluding uniform corrosion. These two parameters can be calculated using pit depth based on geometric relationships.

The pit depth is calculated as

$$p(t) = R\int_{T_i}^{T} r_{corr}(t_p)dt_p \quad (7)$$

where $p(t)$ is the pit depth; and R is the pitting factor. The relationship between uniform corrosion (the depth of uniform corrosion) and pitting corrosion (the maximum pit depth) can be described using the pitting factor. The spatial variability of pitting corrosion can be modelled through the consideration of spatially variant pitting factors. The probabilistic distribution of pitting factors can be determined from experiments. For instance, Extreme Value Type I Gumbel distribution was found to be appropriate to describe the probabilistic distribution of maximum pit depth within every 100 mm length rebar (Stewart and Al-Harthy, 2008).

In addition to area loss of steel, there exist some secondary corrosion effects on reinforced concrete components (Shekhar, Ghosh and Padgett, 2018). For instance, the production of rust lead to an increased volume of corroded steel, the crack of cover concrete appears due to expansion, and loss of cover concrete strength occurs. Similarly, loss of core concrete strength can occur as a result of the corrosion of transverse tie steel. Previous studies found that pitting corrosion can lead to the reduction of yield and ultimate strength of steel (Du, Clark and Chan, 2005; Kashani, Crewe and Alexander, 2013). The effects of corrosion on structures including loss of area of steel and other secondary effects can be modelled using finite element models.

In addition to corrosion, the effects of multiple hazards on structures can also be modelled using finite element models (Li, Dong, Dan M. Frangopol, *et al.*, 2020; Argyroudis and Mitoulis, 2021).

3. Seismic hazard processes

In addition to the corrosion process, the seismic hazard can also affect functionality and resilience within the service life of structures. For long-term performance assessment, earthquakes accruing during the service life of structures should be considered. Within the seismic hazard process, there exist uncertainties associated with both the arrival time of earthquakes and hazard intensities. Earthquake occurrences are normally described using a stochastic process based on historical events. In this section, two stochastic process models of earthquakes including both stationary and nonstationary arrival processes are introduced.

3.1 Stationary arrival process: homogeneous Poisson renewal process

The following considerations apply for the box (5) in Figure 2. The homogeneous Poisson process with stationarity is widely adopted to model the occurrence of earthquakes (Rackwitz, 2002). In this process, the mean occurrence rate is considered as a constant. The probability of n events occurring within the time horizon t_{int} can be expressed as

$$P[N(t_{\text{int}}) = n] = \frac{(\lambda t_{\text{int}})^n \exp(-\lambda t_{\text{int}})}{n!},\ n = 0,1,2,... \tag{8}$$

where λ is the occurrence rate of the event. The homogeneous Poisson process can be considered as a special case of the renewal process. A renewal process can be regarded as a homogeneous Poisson process if an exponential distribution is used to describe the stochastic inter-arrival time, namely the homogeneous Poisson renewal process. In this case, the probability density function (PDF) of waiting time between two successive events is

$$f_W(x_w) = \lambda \exp(-\lambda x_w) \tag{9}$$

3.2 Nonstationary arrival process: Brownian passage-time (BPT) renewal process

The following considerations apply for boxes (4), (5), and (6) in Figure 2. The homogeneous Poisson renewal process adopts the assumption of a constant mean occurrence rate with the time-independent occurrence of hazards. However, there can exist time-dependent features

297 within the occurrence of earthquakes. For instance, a rupture can occur when the stochastic
298 load state process arrives at a certain failure state. The energy is released through the
299 earthquake, and a new cycle of energy accumulation starts. Due to the energy accumulation
300 and release process, the occurrence of earthquakes is associated with time-dependent
301 characteristics. In such a situation, the Brownian passage-time (BPT) renewal process with
302 nonstationary features can be used to predict the long-term occurrence of earthquakes in a
303 time-dependent manner (Matthews, Ellsworth and Reasenberg, 2002; Li, Dong, Dan M
304 Frangopol, *et al.*, 2020). The BPT distribution is used to represent probabilistic inter-arrival time,
305 the PDF of BPT distribution is

306 $$f_W(x_w) = \left(\frac{\mu}{2\pi\alpha^2 t^3}\right)^{1/2} \exp\left\{-\frac{(t-\mu)^2}{2\mu\alpha^2 t}\right\} \quad (10)$$

307 where μ and α are the mean and coefficient of variation, respectively.

308 In addition to the uncertainty associated with the arrival of earthquakes, the earthquake
309 intensity can be uncertain for each event (Qian and Dong, 2020). For a given magnitude, the
310 seismic intensities are considered to follow lognormal distribution (Boore *et al.*, 2014). The
311 ground motion prediction models (GMPMs) are widely adopted to predict the probabilistic
312 hazard intensity levels. The GMPMs provide medians and standard deviations conditioned on
313 earthquake scenario parameters, such as distance, magnitude, rupture mechanism, and others.
314 The GMPM (Boore *et al.*, 2014) is expressed as

315 $$\ln Y = F_E(M, mech) + F_P(R_{JB}, M, region) + F_S(V_{S30}, R_{JB}, M, region, z_1) + \varepsilon\sigma(M, R_{JB}, V_{S30}) \quad (11)$$

316 where $\ln Y$ is the natural logarithm of ground motion intensity; F_E, F_P, and F_S represent functions
317 of source, path, and site parameters respectively; M represents the moment magnitude of the
318 event; *mech* is the earthquake mechanism; R_{JB} is the Joyner-Boore distance; the *region* is the
319 region of the earthquake accruing; V_{S30} is the shear wave velocity averaged over top 30 *m*; z_1 is
320 the basin depth; ε is the fractional number of standard deviations of the value of $\ln Y$ away from
321 the mean; and σ represents the standard deviation of the model.

322 **4. Long-term resilience under compound earthquake and deterioration processes**

To assess long-term resilience, the threats affecting the functionality of structures within the service life should be incorporated. Earthquakes can occur at a stochastic time within the service-life of structures, resulting in a sudden drop in functionality. Furthermore, deterioration due to chloride environment can escalate the damage probability of structures under earthquakes. Thus, the seismic vulnerability should be computed in a time-variant manner considering the deterioration process. Then, long-term resilience can be assessed based on time-variant seismic vulnerability and earthquake processes. The detailed approach is introduced as follows.

4.1 Time-variant seismic vulnerability

The following considerations apply for boxes (7), (8), and (9) in Figure 2. Structures can deteriorate over time, and the demand and capacity of structures can be time-variant, leading to time-variant seismic vulnerability. To assess seismic vulnerability, both probabilistic seismic demand and capacity should be updated from time considering corrosion. The median of seismic demand considering its evolution from time can be written as (Dong, Frangopol and Saydam, 2013)

$$\ln(S_d(t, IM)) = a(t) + b(t) \cdot \ln(IM) \tag{12}$$

where IM is the seismic intensity measure; $S_d(t,IM)$ is the median of seismic demand under given time t and IM; and $a(t)$ and $b(t)$ are the coefficients of the demand prediction model at time t.

For time-variant capacity, the pushover analysis can be performed to determine the capacity of the column under corrosion. Once the probabilistic distributions of structural demand and capacity are determined, a set of demand and capacity samples with respect to different structural components can be generated. The structural system-level binary survive-failure vector can be computed by comparing demand and capacity samples. By using seismic IM and system-level binary survive-failure vector as input, logistic regression can be performed to develop time-variant fragility model of structures (Shekhar, Ghosh and Padgett, 2018; Qian and Dong, 2022). The time-variant fragility model is expressed as (Shekhar, Ghosh and Padgett, 2018)

$$F(IM \mid t, DS) = \frac{e^{\beta_{0,DS}(t)+\beta_{IM,DS}(t)\cdot IM}}{1+e^{\beta_{0,DS}(t)+\beta_{IM,DS}(t)\cdot IM}} \quad (13)$$

where $F(IM|t,DS)$ represents the fragility of the structure under IM and damage state DS at time t; and $\beta_{0,DS}(t)$ and $\beta_{IM,DS}(t)$ are the coefficients of the logistic regression at time t. The procedures of developing time-variant fragility are presented in Figure 1.

4.2 Long-term resilience assessment

The following considerations apply for boxes (10), (11), and (12) in Figure 2. Based on the concept of resilience loss (Bocchini *et al.*, 2014; Yang and Frangopol, 2019), the resilience loss index is defined as

$$R_L(t_i) = \frac{t_h \cdot 100\% - \int_{t_i}^{t_i+t_h} Q(t \mid t_i)dt}{t_h} \quad (14)$$

where $R_L(t_i)$ is the resilience loss index caused by the earthquake at time t_i; t_h is the investigated recovery time horizon; and $Q(t|t_i)$ is the post-hazard time-variant functionality of the system under the earthquake accruing at time t_i. As indicated in Eq. 14, time-variant functionality of the system is essential for computation of resilience loss. To illustrate the proposed framework, this study adopts a cumulative distribution function to model the time-variant functionality of bridges (ATC, 1999; HAZUS, 2010). There also exist some other time-variant functionality models to describe the recovery process, such as the stepwise model (Padgett and DesRoches, 2007), the six-parameter probabilistic restoration model (Decò, Bocchini and Frangopol, 2013), and exponential model (Chang and Shinozuka, 2004). Given different time-variant functionality models incorporating different aspects, the results of resilience loss can be updated using the proposed framework. Given the occurrence time and intensity of earthquakes from seismic process model, the probabilities of bridges being in each damage state can be computed based on the time-variant fragility model. The expected time-variant functionality is calculated as the sum of weighted functionalities associated with each damage state, using the corresponding probabilities as weightings.

Several earthquakes may occur during the service life of structures. The long-term resilience loss can be computed as the accumulation of all potential resilience losses within the investigated time horizon as (Yang and Frangopol, 2019)

$$L_R = \sum_{k=1}^{N_h(t_L)} R_L(t_i) \quad (15)$$

where L_R is the long-term resilience loss; t_L is the investigated time horizon; and $N_h(t_L)$ is the number of hazards within the investigated time horizon.

This study proposes a framework for long-term resilience assessment considering compound earthquake and deterioration processes. The developed framework is presented in Figure 2. As illustrated, the framework consists of four components: deterioration process module, hazard process module, time-variant fragility module, and long-term resilience loss module. In the deterioration process module, primary and secondary effects of corrosion on structures (Eqs. 5-7) are modelled given the environmental exposure (Eqs. 1-4) and corresponding probabilistic parameters. In the hazard process module, the occurrence of earthquakes in a long-term perspective is modelled using stochastic process theory (Eqs. 8-10), and the probabilistic hazard intensity can be computed from the ground motion prediction model (Eq. 11). The time-variant seismic fragility incorporating corrosion effects is developed considering time-variant demand and capacity (Eqs. 12-13). By using the above three modules, the computation of long-term resilience can be formulated. A set of earthquake events with stochastic occurrence time and intensity are simulated from the hazard process module (Eqs. 8-11). Then, the time-variant functionality and resilience loss under simulated events can be computed (Eqs. 13-14). Finally, long-term resilience loss can be computed as the accumulation of resilience losses within the investigated time horizon (Eq. 15). An illustrative example of long-term resilience under seismic and deterioration processes is shown in Figure 3.

5. Illustrative example

To assess long-term resilience, the corrosion effects on bridges should be modelled based on identified exposure environment. Then, time-variant fragility is computed considering time-variant demand and capacity. A set of earthquake realizations with stochastic occurrence time and intensity is simulated from the earthquake process model. Finally, the long-term resilience

loss is computed by accumulating resilience losses induced by all potential events within the investigated time interval.

Shekhar, Ghosh and Padgett, (2018) modelled the effects of corrosion on bridges including pitting corrosion and other secondary effects, and both demand and capacity models were developed in a time-variant manner. The time-variant fragility model under deicing salt exposure conditions (Shekhar, Ghosh and Padgett, 2018) is adopted in this case study. The fragility curves associated with slight, moderate, extensive, and complete damage states for the pristine bridge are presented in Figure 4. By considering deterioration, the time-variant fragility curves for the complete damage state are illustrated in Figure 5. As indicated, the pristine bridge is associated with the lowest damage probability, and the damage probability increases significantly over time. The deterioration process can significantly affect the seismic vulnerability of bridges.

Multiple earthquakes can occur during the service life of structures. The stochastic occurrence time of earthquake serves as the input of time-variant fragility. In the meanwhile, the seismic intensity can be random for each earthquake event, and probabilistic seismic intensity can be computed using the ground motion prediction model (Boore *et al.*, 2014). Given the information of occurrence time and intensity of hazard, vulnerability can be computed from the time-variant fragility model. Then, resilience losses for all earthquakes occurring within the investigated time horizon can be computed, and long-term resilience loss is obtained by accumulating all the resilience losses. To incorporate the uncertainties associated with the occurrence time of earthquakes, deterioration, and seismic intensity, the simulation method is used in this study to compute probabilistic long-term resilience loss. The earthquake magnitude is considered as 7.5. The corresponding parameters associated with seismic processes are adopted from Pandey and Van Der Weide (2017). An illustrative realization of long-term resilience simulation is shown in Figure 6. The earthquakes can occur at time t_1, t_2, t_3,…, and t_k, where the inter-arrival time W_1, W_2, W_3,…, and W_k can be generated from probabilistic distribution associated with the renewal process. Considering deterioration, the vulnerability of structures at the time of different earthquake events can be determined from the time-variant fragility model as V_{t1}, V_{t2}, V_{t3},…, and V_{tk}. The resilience loss $R_L(t_1)$, $R_L(t_2)$, $R_L(t_3)$,…, and $R_L(t_k)$

associated with all earthquakes can be computed. Finally, long-term resilience loss is computed by the accumulation of all resilience losses. A total of 5×10^5 simulations are carried out to compute probabilistic long-term resilience loss.

In this study, the effects of the corrosion process and different earthquake processes (e.g., HPP and BPT) on long-term resilience loss are investigated. The PDFs of inter-arrival time associated with HPP and BPT are presented in Figure 7. Different distribution shapes are observed, different seismic processes can significantly affect the probabilistic distribution of inter-arrival time. The mean values and standard deviations of long-term resilience loss under different process combinations are illustrated in Figures 8 and 9, respectively. By considering both corrosion and earthquake processes, the mean of long-term resilience loss associated with long period increases significantly compared with those associated with the earthquake process. The standard deviation of long-term resilience loss under both corrosion and earthquake processes is higher than the one under a sole earthquake process, indicating a larger level of uncertainty. The corrosion process induces additional uncertainty for long-term resilience. Under the same corrosion process, HPP and BPT produce different results in terms of the mean and standard deviation of long-term resilience loss. The statistical moments of long-term resilience loss under a time horizon of 75 years are presented in Table 1. The significant difference of statistical moments of long-term resilience loss is observed by using different process models. These results highlight the importance of considering the deterioration process as well as choosing an appropriate earthquake process model for long-term resilience assessment. As indicated previously, HPP is a stationary process with a constant mean occurrence rate, and the occurrence of hazards is considered as time-independent. The BPT process model is a nonstationary model which incorporates the consideration of energy accumulation and release process. The time-variant characteristics of the occurrence of earthquakes can be modelled using the BPT model.

Table 1. Statistical moments of long-term resilience loss under time horizon of 75 years

Dependence model	Mean	STD	Skewness	Kurtosis
HPP	0.12	0.15	2.10	8.63
BPT	0.10	0.12	2.27	9.37
HPP; corrosion	0.30	0.32	1.43	5.30
BPT; corrosion	0.27	0.25	1.07	3.79

The workflow of long-term resilience loss assessment with respect to boxes of Figure 2 is listed in Table 2.

Table 2. workflow of long-term resilience loss assessment

The number of boxes	workflow	Equations
(1)	Determine exposure environment	
(2)	Determine exposure environment parameters	(1)-(4)
(3)	Model corrosion effects	(5)-(7)
(4)	Identify earthquake scenario	
(5)	Determine stochastic process of earthquakes	(8)-(10)
(6)	Determine ground motion prediction model	(11)
(7)	Assess time-variant seismic demand	(12)
(8)	Assess time-variant seismic capacity	
(9)	Develop time-variant seismic fragility model	(13)
(10)	Simulate stochastic earthquake events	(8)-(11)
(11)	Compute functionality and resilience loss	(13)-(14)
(12)	Compute long-term resilience loss	(15)

This study focuses on developing a general framework for long-term resilience assessment under seismic and deterioration processes. Resilience can be assessed periodically. For instance, the data from periodic inspections and structural health monitoring can be used to update the resilience timely. The resilience assessment can also be updated after each extreme event (e.g., earthquake) by incorporating the post-event structural effects.

6. Conclusions

This study develops a framework for long-term resilience assessment of structures under time-dependent seismic and deterioration processes. The effects of the deterioration process on structures lead to time-variant seismic demand and capacity. The time-variant fragility model can be developed considering the deterioration process. Two earthquake process models are introduced, namely HPP and BPT. The occurrence time and intensity of earthquakes within the investigated time horizon can be simulated from the stochastic process model and ground

motion prediction model, respectively. Based on the earthquake process model and time-variant fragility model, long-term resilience loss can be computed by accumulating the resilience losses induced from all earthquakes within the investigated time horizon. The obtained results can benefit decision-making and adaptation measures in real-life problems. In the design stage, structures can be optimized based on the considered long-term resilience threshold. In the operational stage, the decision can be made to select the optimal adaptation measure (e.g., retrofit) based on quantified long-term resilience. When risk aversion is considered within the decision-making of structures, the decision-makers can consider different decision attitudes by using high order moments of long-term resilience (e.g., variance, skewness, and kurtosis), which can be computed from probabilistic distribution. The following conclusions are drawn:

- The deterioration process can significantly increase the seismic vulnerability and long-term resilience loss within the service life of structures. The consideration of the deterioration process is of vital importance for accurate long-term resilience assessment.
- By considering the deterioration process, a larger amount of uncertainty for long-term resilience loss is observed compared with the case associated with a sole earthquake process.
- The stationary model HPP adopts the assumption of time-independent occurrence of hazards. However, the time-dependent features of the occurrence of earthquakes can be modelled by the BPT process model.
- The difference between the statistical moments of long-term resilience loss is large by using different earthquake process models, indicating the importance of appropriate modelling of time-dependent characteristics of hazard and choice of the hazard process model.
- The developed approach contributes to the resilience assessment in a long-term perspective, incorporating time-varying characteristics associated with both earthquakes and deterioration. The uncertainties associated with the occurrence time of hazard, hazard intensity, deterioration, and structural damage are incorporated in the developed framework.

Acknowledgements

The study has been supported by the National Natural Science Foundation of China (grant no. 51808476 and 52078448) and the Research Grant Council of Hong Kong (PolyU 15219819). The support is gratefully acknowledged. The opinions and conclusions presented in this paper are those of the authors and do not necessarily reflect the views of the sponsoring organizations.

References

ATC. (1999) Earthquake damage evaluation data for California. Technical Report ATC-13, Applied Technology Council, Redwood City, CA.

Akiyama, M., Frangopol, D. M. and Ishibashi, H. (2020) 'Toward life-cycle reliability-, risk-and resilience-based design and assessment of bridges and bridge networks under independent and interacting hazards: emphasis on earthquake, tsunami and corrosion', *Structure and Infrastructure Engineering*. Taylor & Francis, 16(1), pp. 26–50.

Argyroudis, S. A. *et al.* (2020) 'Resilience assessment framework for critical infrastructure in a multi-hazard environment: Case study on transport assets', *Science of The Total Environment*. Elsevier, 714, p. 136854.

Argyroudis, S. A. and Mitoulis, S. A. (2021) 'Vulnerability of bridges to individual and multiple hazards-floods and earthquakes', *Reliability Engineering & System Safety*. Elsevier, 210, p. 107564.

Bocchini, P., Frangopol, D. M., Ummenhofer, T. and Zinke, T. (2014) 'Resilience and sustainability of civil infrastructure: Toward a unified approach', *Journal of Infrastructure Systems*. American Society of Civil Engineers, 20(2), p. 4014004.

Boore, D. M., Stewart, J. P., Seyhan, E., and Atkinson, G. M (2014) 'NGA-West2 equations for predicting PGA, PGV, and 5% damped PSA for shallow crustal earthquakes', *Earthquake Spectra*. Earthquake Engineering Research Institute, 30(3), pp. 1057–1085.

Capacci, L. and Biondini, F. (2020) 'Probabilistic life-cycle seismic resilience assessment of aging bridge networks considering infrastructure upgrading', *Structure and Infrastructure Engineering*. Taylor & Francis, 16(4), pp. 659–675. doi: 10.1080/15732479.2020.1716258.

534 Chang, S. E. and Shinozuka, M. (2004) ‘Measuring improvements in the disaster resilience of
535 communities’, *Earthquake spectra*. SAGE Publications Sage UK: London, England, 20(3), pp.
536 739–755.

537 Choe, D.-E. *et al.* (2008) ‘Probabilistic capacity models and seismic fragility estimates for RC
538 columns subject to corrosion’, *Reliability Engineering & System Safety*. Elsevier, 93(3), pp. 383–
539 393.

540 Decò, A., Bocchini, P. and Frangopol, D. M. (2013) ‘A probabilistic approach for the prediction of
541 seismic resilience of bridges’, *Earthquake Engineering and Structural Dynamics*, Wiley, 42(10),
542 pp. 1469–1487. doi: 10.1002/eqe.

543 Dong, Y. and Frangopol, D. M. (2015) ‘Risk and resilience assessment of bridges under
544 mainshock and aftershocks incorporating uncertainties’, *Engineering Structures*. Elsevier Ltd, 83,
545 pp. 198–208. doi: 10.1016/j.engstruct.2014.10.050.

546 Dong, Y. and Frangopol, D. M. (2016) ‘Probabilistic time-dependent multihazard life-cycle
547 assessment and resilience of bridges considering climate change’, *Journal of Performance of
548 Constructed Facilities*. American Society of Civil Engineers, 30(5), p. 4016034.

549 Dong, Y., Frangopol, D. M. and Saydam, D. (2013) ‘Time-variant sustainability assessment of
550 seismically vulnerable bridges subjected to multiple hazards’, *Earthquake Engineering &
551 Structural Dynamics*. Wiley Online Library, 42(10), pp. 1451–1467.

552 Du, Y. G., Clark, L. A. and Chan, A. H. C. (2005) ‘Residual capacity of corroded reinforcing bars’,
553 *Magazine of Concrete Research*. Thomas Telford Ltd, 57(3), pp. 135–147.

554 Engelund, S., Edvardsen, C. and Mohr, L. (2000) ‘General guidelines for durability design and
555 redesign’, *Report R15 of EU-Brite EuRam III project BE95-1347 DuraCrete. Probabilistic
556 performance based durability design of concrete structures*.

557 Enright, M. P. and Frangopol, D. M. (1998) ‘Probabilistic analysis of resistance degradation of
558 reinforced concrete bridge beams under corrosion’, *Engineering structures*. Elsevier, 20(11), pp.
559 960–971.

Frangopol, D. M. and Bocchini, P. (2011) ‘Resilience as optimization criterion for the rehabilitation of bridges belonging to a transportation network subject to earthquake’, in *Structures Congress 2011*, pp. 2044–2055.

Frangopol, D. M., Lin, K.-Y. and Estes, A. C. (1997) ‘Reliability of reinforced concrete girders under corrosion attack’, *Journal of Structural Engineering*. American Society of Civil Engineers, 123(3), pp. 286–297.

Ghosh, J. and Padgett, J. E. (2010) ‘Aging considerations in the development of time-dependent seismic fragility curves’, *Journal of Structural Engineering*. American Society of Civil Engineers, 136(12), pp. 1497–1511.

Ghosh, J. and Padgett, J. E. (2012) ‘Impact of multiple component deterioration and exposure conditions on seismic vulnerability of concrete bridges’, *Earthquakes and Structures*. Techno-Press, 3(5), pp. 649–673.

Ghosh, J. and Sood, P. (2016) ‘Consideration of time-evolving capacity distributions and improved degradation models for seismic fragility assessment of aging highway bridges’, *Reliability Engineering & System Safety*. Elsevier, 154, pp. 197–218.

HAZUS-MH (2010) Multi-hazard loss estimation methodology—earthquake model (technical manual). Technical Report MH MR5, Federal Emergency Management Agency, Washington.

Kashani, M. M., Crewe, A. J. and Alexander, N. A. (2013) ‘Nonlinear stress--strain behaviour of corrosion-damaged reinforcing bars including inelastic buckling’, *Engineering Structures*. Elsevier, 48, pp. 417–429.

Kong, J. and Simonovic, S. P. (2019) ‘Probabilistic multiple hazard resilience model of an interdependent infrastructure system’, *Risk Analysis*. Wiley Online Library, 39(8), pp. 1843–1863.

Li, Y., Dong, Y., Frangopol, D. M. and Gautam, D. (2020) ‘Long-term resilience and loss assessment of highway bridges under multiple natural hazards’, *Structure and Infrastructure Engineering*. Taylor & Francis, 16(4), pp. 626–641.

586 Liu, M., Wen, Y. K. and Burns, S. A. (2004) ‘Life cycle cost oriented seismic design optimization
587 of steel moment frame structures with risk-taking preference’, *Engineering Structures*. Elsevier,
588 26(10), pp. 1407–1421.

589 Matthews, M. V, Ellsworth, W. L. and Reasenberg, P. A. (2002) ‘A Brownian model for recurrent
590 earthquakes’, *Bulletin of the Seismological Society of America*. Seismological Society of
591 America, 92(6), pp. 2233–2250.

592 Minaie, E. and Moon, F. (2017) ‘Practical and simplified approach for quantifying bridge
593 resilience’, *Journal of Infrastructure Systems*, 23(4), pp. 1–11. doi: 10.1061/(ASCE)IS.1943-
594 555X.0000374.

595 Padgett, J. E. and DesRoches, R. (2007) ‘Bridge functionality relationships for improved seismic
596 risk assessment of transportation networks’, *Earthquake Spectra*. SAGE Publications Sage UK:
597 London, England, 23(1), pp. 115–130.

598 Pandey, M. D. and Van Der Weide, J. A. M. (2017) ‘Stochastic renewal process models for
599 estimation of damage cost over the life-cycle of a structure’, *Structural Safety*. Elsevier, 67, pp.
600 27–38.

601 Qian, J. and Dong, Y. (2020) ‘Multi-criteria decision making for seismic intensity measure
602 selection considering uncertainty’, *Earthquake Engineering and Structural Dynamics*, (March),
603 pp. 1–20. doi: 10.1002/eqe.3280.

604 Qian, J. and Dong, Y. (2022) ‘Uncertainty and multi-criteria global sensitivity analysis of
605 structural systems using acceleration algorithm and sparse polynomial chaos expansion’,
606 *Mechanical Systems and Signal Processing*. Elsevier, 163, p. 108120.

607 Rackwitz, R. (2002) ‘Optimization and risk acceptability based on the life quality index’,
608 *Structural safety*. Elsevier, 24(2–4), pp. 297–331.

609 Shekhar, S., Ghosh, J. and Padgett, J. E. (2018) ‘Seismic life-cycle cost analysis of ageing
610 highway bridges under chloride exposure conditions: Modelling and recommendations’,
611 *Structure and Infrastructure Engineering*. Taylor & Francis, 14(7), pp. 941–966.

612 Stewart, M. G. and Al-Harthy, A. (2008) ‘Pitting corrosion and structural reliability of corroding
613 RC structures: Experimental data and probabilistic analysis’, *Reliability Engineering & System*
614 *Safety*. Elsevier, 93(3), pp. 373–382.

615 Takahashi, Y., Kiureghian, A. Der and Ang, A. H.-S. (2004) ‘Life-cycle cost analysis based on a
616 renewal model of earthquake occurrences’, *Earthquake engineering & structural dynamics*.
617 Wiley Online Library, 33(7), pp. 859–880.

618 Timmerman, P. (1981) ‘Vulnerability resilience and collapse ofsociety’, *A ReviewofModels and*
619 *Possible Climatic Appli-cations. Toronto, Canada. Institute for Environmental Studies, University*
620 *of Toronto*.

621 Vu, K. A. T. and Stewart, M. G. (2000) ‘Structural reliability of concrete bridges including
622 improved chloride-induced corrosion models’, *Structural safety*. Elsevier, 22(4), pp. 313–333.

623 Yang, D. Y. and Frangopol, D. M. (2019) ‘Life-cycle management of deteriorating civil
624 infrastructure considering resilience to lifetime hazards: A general approach based on renewal-
625 reward processes’, *Reliability Engineering & System Safety*. Elsevier, 183, pp. 197–212.

626 Zandi Hanjari, K., Kettil, P. and Lundgren, K. (2011) ‘Analysis of mechanical behavior of
627 corroded reinforced concrete structures’, *ACI Structural Journal*, 108(5), pp. 532–541.

628 **Figure captions (images as individual files separate to your MS Word text file).**

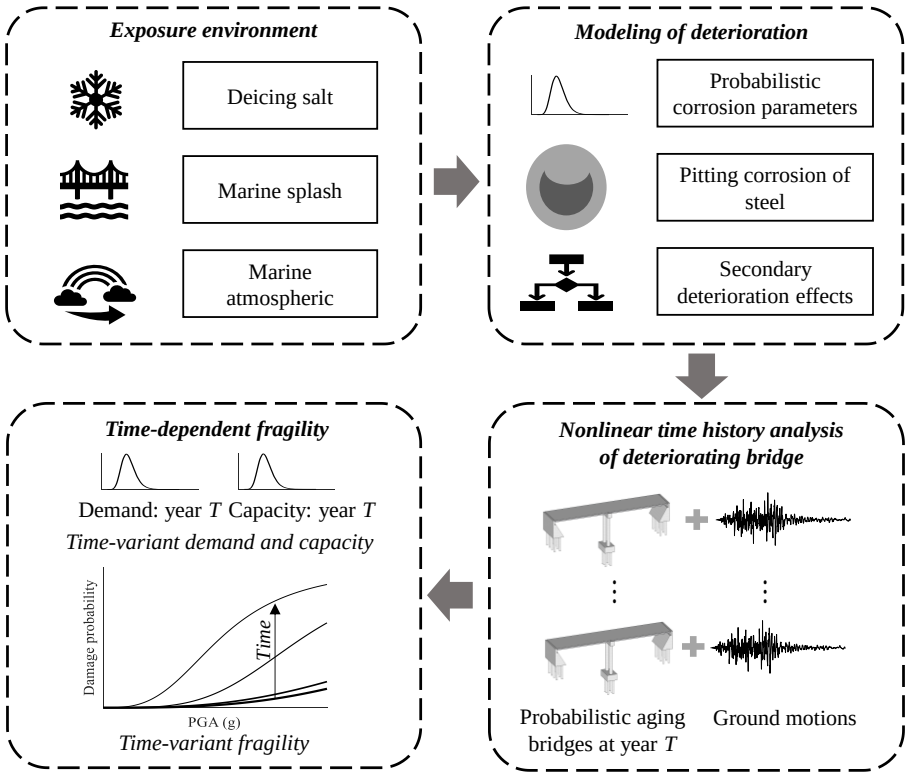

Figure 1. Framework of developing time-dependent fragility

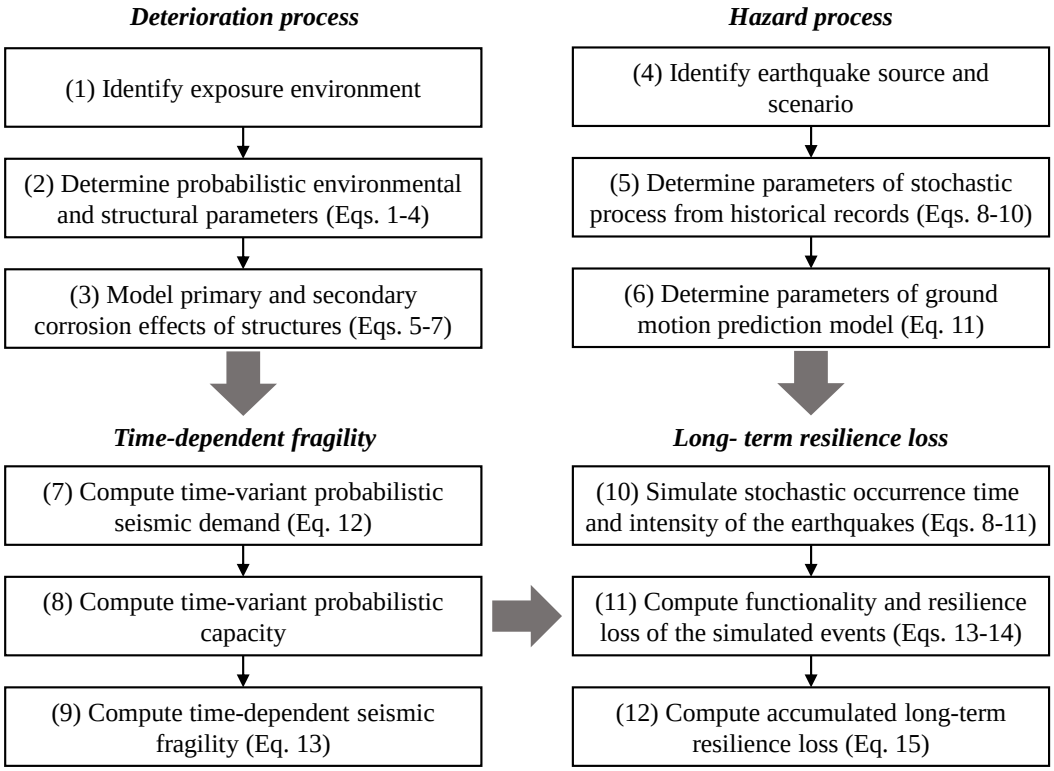

Figure 2. Framework of long-term resilience assessment under seismic and deterioration processes

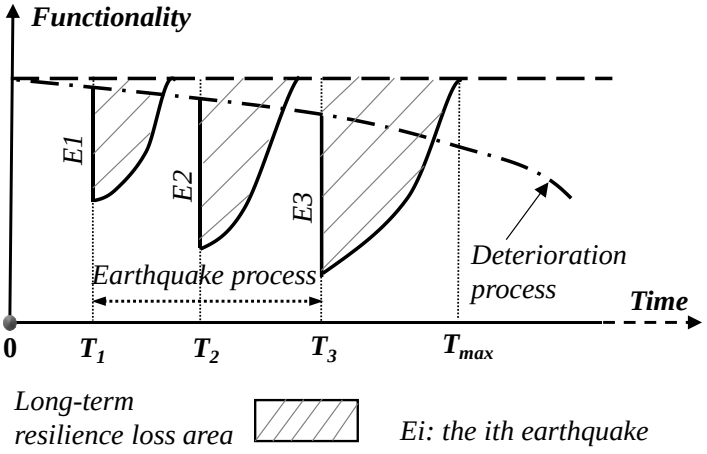

Figure 3. Illustration of long-term resilience under seismic and deterioration processes

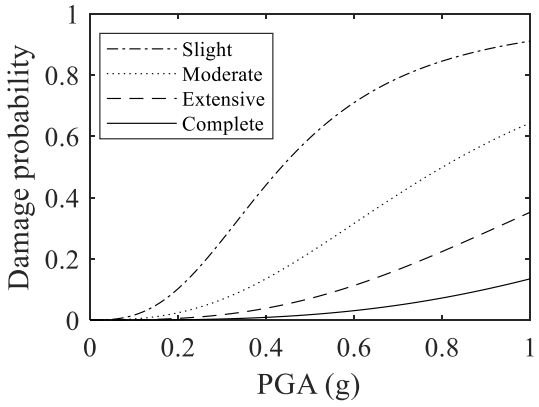

Figure 4. Seismic fragility curves of pristine bridge associated with four damage states

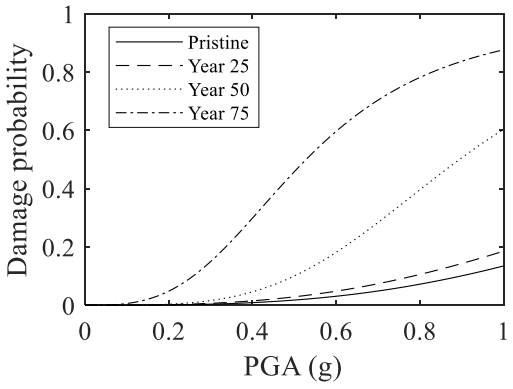

Figure 5. Seismic fragility curves of the pristine bridge and deteriorating bridge for complete damage state

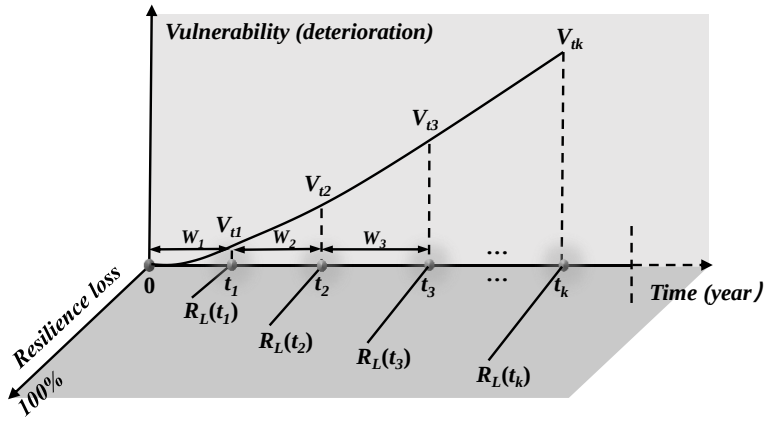

645

646 Figure 6. Illustration of long-term resilience simulation under seismic and deterioration
647 processes

648

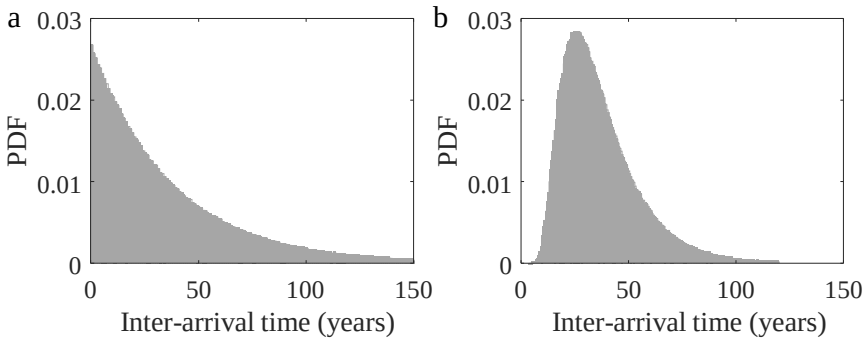

649

650 Figure 7. Probability density functions of inter-arrival time associated with (a) HPP and (b) BPT

651

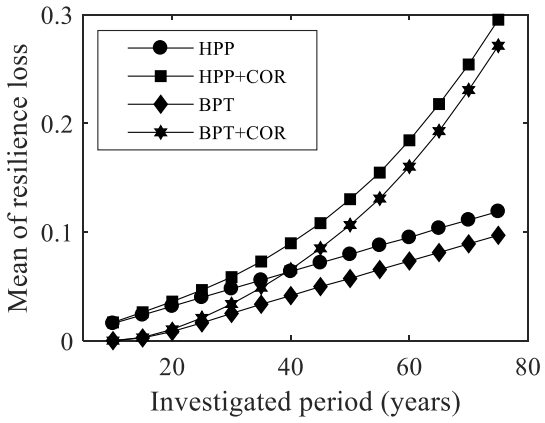

652

653 Figure 8. Mean value of long-term resilience under different processes

654

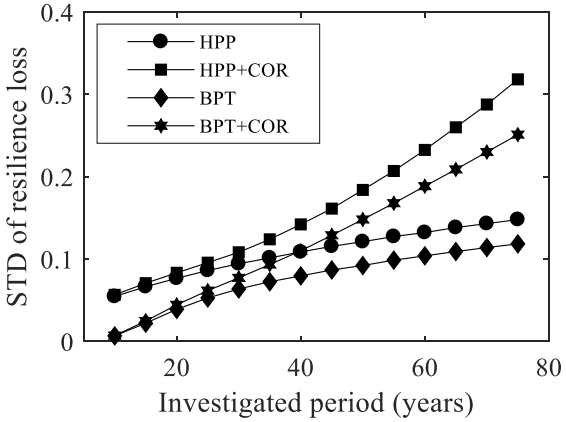

655

656 Figure 9. Standard deviation (STD) of long-term resilience under different processes